Overexpression of Arabidopsis Ceramide Synthases Differentially Affects Growth, Sphingolipid Metabolism, Programmed Cell Death, and Mycotoxin Resistance[1][OPEN]

Kyle D. Luttgeharm, Ming Chen, Amit Mehra, Rebecca E. Cahoon, Jonathan E. Markham, and Edgar B. Cahoon*

Center for Plant Science Innovation and Department of Biochemistry, University of Nebraska-Lincoln, Nebraska 68588

ORCID ID: 0000-0002-7277-1176 (E.B.C.).

Ceramide synthases catalyze an *N*-acyltransferase reaction using fatty acyl-coenzyme A (CoA) and long-chain base (LCB) substrates to form the sphingolipid ceramide backbone and are targets for inhibition by the mycotoxin fumonisin B_1 (FB_1). Arabidopsis (*Arabidopsis thaliana*) contains three genes encoding ceramide synthases with distinct substrate specificities: *LONGEVITY ASSURANCE GENE ONE HOMOLOG1* (*LOH1*; At3g25540)- and *LOH3* (At1g19260)-encoded ceramide synthases use very-long-chain fatty acyl-CoA and trihydroxy LCB substrates, and *LOH2* (At3g19260)-encoded ceramide synthase uses palmitoyl-CoA and dihydroxy LCB substrates. In this study, complementary DNAs for each gene were overexpressed to determine the role of individual isoforms in physiology and sphingolipid metabolism. Differences were observed in growth resulting from *LOH1* and *LOH3* overexpression compared with *LOH2* overexpression. *LOH1*- and *LOH3*-overexpressing plants had enhanced biomass relative to wild-type plants, due in part to increased cell division, suggesting that enhanced synthesis of very-long-chain fatty acid/trihydroxy LCB ceramides promotes cell division and growth. Conversely, *LOH2* overexpression resulted in dwarfing. *LOH2* overexpression also resulted in the accumulation of sphingolipids with C16 fatty acid/dihydroxy LCB ceramides, constitutive induction of programmed cell death, and accumulation of salicylic acid, closely mimicking phenotypes observed previously in LCB C-4 hydroxylase mutants defective in trihydroxy LCB synthesis. In addition, *LOH2*- and *LOH3*-overexpressing plants acquired increased resistance to FB_1, whereas *LOH1*-overexpressing plants showed no increase in FB_1 resistance, compared with wild-type plants, indicating that *LOH1* ceramide synthase is most strongly inhibited by FB_1. Overall, the findings described here demonstrate that overexpression of Arabidopsis ceramide synthases results in strongly divergent physiological and metabolic phenotypes, some of which have significance for improved plant performance.

Ceramides are central intermediates in sphingolipid biosynthesis and mediators of programmed cell death (PCD) in plants (Dunn et al., 2004; Saucedo-García et al., 2011; Ternes et al., 2011a). Ceramides are synthesized by ceramide synthase (or sphingosine *N*-acyltransferase; EC 2.3.1.24), which catalyzes the formation of an amide linkage between a sphingoid long-chain base (LCB) and a fatty acid using LCB and fatty acyl-CoA substrates (Mullen et al., 2012). The LCB substrate can have two or three hydroxyl groups that are referred to as dihydroxy or trihydroxy LCBs, respectively (Chen et al., 2010). The fatty acyl-CoA substrates typically have chain lengths of C16 or C22 to C26 (Dunn et al., 2004). The latter are referred to as very-long-chain fatty acids (VLCFAs). The ceramide product of ceramide synthase is used primarily as a substrate for the synthesis of either of the two major glycosphingolipids found in plants: glucosylceramide (GlcCer) and glycosyl inositolphosphoceramide (GIPC; Chen et al., 2010). These glycosphingolipids are major structural components of the plasma membrane and other endomembranes of plant cells (Verhoek et al., 1983; Sperling et al., 2005). In this role, they contribute to membrane physical properties that are important for the ability of plant cells to adjust to environmental extremes and to Golgi-mediated protein trafficking of proteins, including cell wall metabolic enzymes and auxin transporters that underlie plant growth (Borner et al., 2005; Markham et al., 2011; Mortimer et al., 2013; Yang et al., 2013). Alternatively, ceramides can be converted to ceramide-1-phosphates by ceramide kinase activity

(Liang et al., 2003). The interchange of ceramides between their free and phosphorylated forms has been linked to the regulation of PCD and PCD-associated resistance to pathogens via the hypersensitive response (HR; Liang et al., 2003; Bi et al., 2014; Simanshu et al., 2014).

The Arabidopsis (*Arabidopsis thaliana*) genome contains three ceramide synthase genes denoted *LONGEVITY ASSURANCE GENE ONE HOMOLOG1* (*LOH1*; At3g25540), *LOH2* (At3g19260), and *LOH3* (At1g13580; Markham et al., 2011; Ternes et al., 2011a). These studies suggest that LOH1 and LOH3 polypeptides are structurally related and catalyze primarily the amidation reaction of trihydroxy LCBs and CoA esters of VLCFAs. The LOH2 polypeptide is more distantly related to LOH1 and LOH3 and catalyzes primarily the condensation of dihydroxy LCBs and C16 fatty acyl-CoAs (Chen et al., 2008; Markham et al., 2011; Ternes et al., 2011a). The ceramide products of LOH1 and LOH3 are most prevalent in GIPC, whereas the ceramide products of LOH2 are more enriched in GlcCer (Markham and Jaworski, 2007; Chen et al., 2008; Ternes et al., 2011b). Similar to plants, the six ceramide synthase isoforms found in humans and mice have distinct specificities for their LCB and acyl-CoA substrates, and these specificities contribute to the formation of complex sphingolipids with differing structures and functions (Venkataraman et al., 2002; Riebeling et al., 2003; Mizutani et al., 2005, 2006; Laviad et al., 2008).

In Arabidopsis, *LOH1* and *LOH3* are partially redundant, but the combined activities of the corresponding polypeptides are essential for plant cell viability, as null double mutants of these genes are lethal (Markham et al., 2011). In contrast, mutants of *LOH2* are viable and display no apparent growth phenotype, which brings into question the role of LOH2 ceramide synthase in plant performance (Markham et al., 2011; Ternes et al., 2011a). Overall, these observations indicate that sphingolipids with LOH1-/LOH3-derived trihydroxy LCBs and VLCFA ceramides are essential, but LOH2-derived dihydroxy LCBs and C16 fatty acid ceramides are not required by plant cells. Related to this, LCB C-4 hydroxylase mutants that are deficient in trihydroxy LCBs accumulate elevated amounts of sphingolipids with dihydroxy LCB- and C16 fatty acid-containing ceramides via LOH2 activity (Chen et al., 2008). These mutants are severely impaired in growth and do not transition from vegetative to reproductive growth (Chen et al., 2008).

Ceramide synthases are known targets for competitive inhibition by sphingosine analog mycotoxins, including fumonisin B_1 (FB_1) and AAL toxin, produced by pathogenic fungi such as various *Fusarium* spp. and
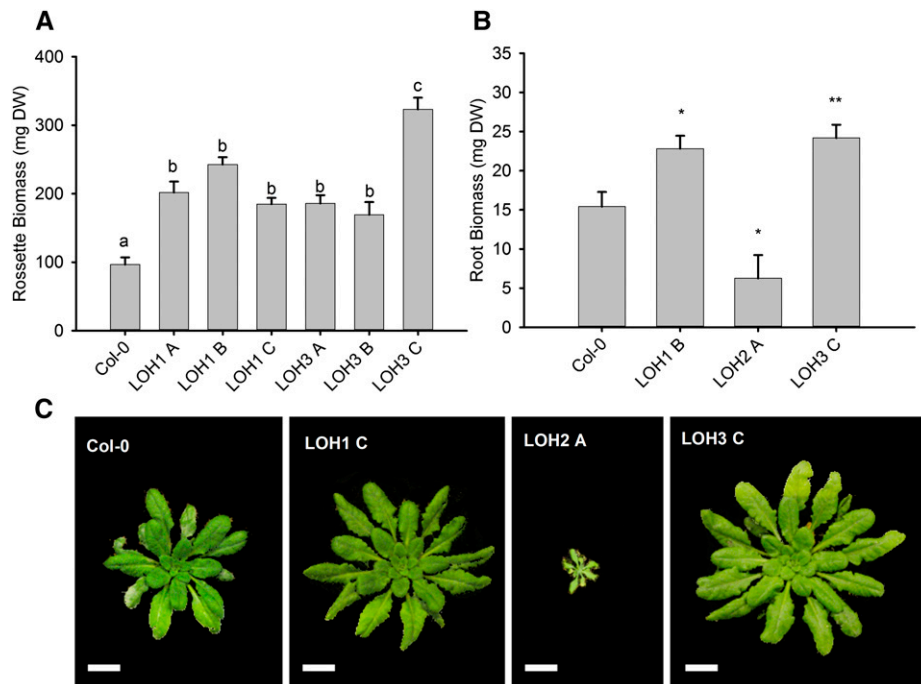
Figure 1. Comparison of rosette and root biomasses in ceramide synthase overexpression lines. A, Dry weights of rosettes from 4-week-old plants presented as the average of independent plants (n = 23 for the wild type [Col-0] and n = 12 for all overexpression lines; lines with the same letter are not significantly different at $P < 0.05$ by Tukey's test) ± SE ($P = 0.00$ for LOH1 line A, LOH1 line B, LOH1 line C, LOH3 line A, LOH3 line B, and LOH3 line C compared with Col-0). B, Dry weights of roots from hydroponically grown plants presented as the average of independent plants (n = 6 for the wild type [Col-0], n = 3 for LOH1 line B, n = 3 for LOH2 line A, and n = 7 for LOH3 line C; *, $P < 0.05$ and **, $P < 0.01$; LOH1 line B, $P = 0.04$; LOH2 line A, $P = 0.03$; and LOH3 line C, $P = 0.005$). Data presented in A and B were obtained from independent transgenic events as indicated in the line nomenclature. DW, Dry weight. C, Representative rosettes from overexpression lines of *LOH1*, *LOH2*, and *LOH3*. Bars = 2 cm.
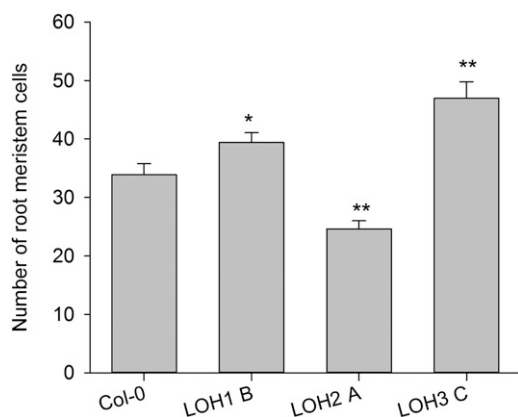
Figure 2. Comparison of epidermal cell numbers in the root meristematic region of ceramide synthase overexpression lines. Epidermal cell numbers were counted in the root meristems of 10 plants from the wild type (Col-0) and representative overexpression lines. Data shown are averages ($n = 10$) ± SE (*, $P < 0.05$ and **, $P < 0.01$; $P = 0.044$, LOH1 line B; $P = 0.00$, LOH2 line A; $P = 0.0011$, LOH3 line C).

Alternaria alternata f. sp. *lycopersici* (Abbas et al., 1994). Inhibition of ceramide synthase results in the accumulation of LCBs that are believed to trigger PCD and result in cytotoxicity (Abbas et al., 1994). In studies of *LOH* mutants, treatment of Arabidopsis seedlings with FB_1 resulted in not only increases in LCBs but also increases in C16 fatty acid-containing sphingolipids and decreases in VLCFA-containing sphingolipids (Markham et al., 2011; Ternes et al., 2011a). The interpretation of this observation was that FB_1 preferentially inhibits LOH1 and LOH3 ceramide synthases but inhibits LOH2 ceramide synthase to a lesser extent (Markham et al., 2011; Ternes et al., 2011a).

Given the findings from Arabidopsis mutants that LOH1 and LOH3 ceramide synthases have distinct substrate specificities and sensitivity to FB_1 relative to LOH2, we hypothesized that the overexpression of each of these ceramide synthases would lead to the production of different sphingolipid compositions as well as different growth phenotypes. This report details experiments designed to test this hypothesis. Among the results presented is a large divergence in the effects of the overexpression of *LOH1* and *LOH3* versus *LOH2* on the growth of Arabidopsis. *LOH2* overexpression was also shown to result in sphingolipid compositional, growth, and physiological phenotypes that closely mimic those observed previously in LCB C-4 hydroxylase mutants (Chen et al., 2008).

RESULTS

Overexpression of LOH1, LOH2, and LOH3 in Arabidopsis Results in Differentially Altered Growth

LOH1, *LOH2*, or *LOH3* complementary DNAs (cDNAs) were expressed under the control of the cauliflower mosaic virus (CaMV) 35S promoter in wild-type

(Columbia-0 [Col-0]) Arabidopsis. From up to 10 independent transgenic lines generated for each cDNA, three lines were selected for further characterization based on confirmed overexpression of the cDNAs as determined by quantitative reverse transcription (RT)-PCR or northern-blot analysis (Supplemental Fig. S1). These lines were taken to homozygosity prior to quantitative measurement of growth and sphingolipid profiles.
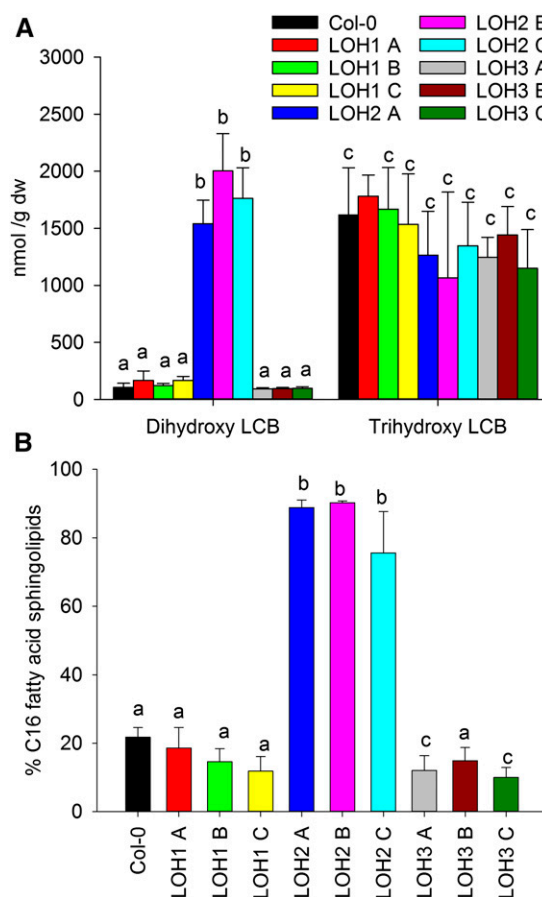
Figure 3. Comparison of concentrations of LCBs and C16 fatty acids in total sphingolipids from 4-week-old rosettes of wild-type plants (Col-0) and *LOH1*, *LOH2*, and *LOH3* overexpression lines. A, Comparison of concentrations of total dihydroxy and trihydroxy LCBs in Col-0 and plants from independent transgenic lines, as indicated by the line nomenclature. Data presented are from measurements of total LCBs measured by HPLC following hydrolysis of sphingolipids in rosettes. Only *LOH2* overexpression lines showed any differences in LCB levels. Data shown are averages of measurements of three independent plants ± SD, and lines with the same letter are not significantly different at $P < 0.05$ by Tukey's test ($P = 0.00$ for all LOH2 lines compared with Col-0 by Tukey's test). B, Percentage of total sphingolipids containing a C16 fatty acid in ceramide backbones as determined by liquid chromatography-electrospray ionization-tandem mass spectrometry. Measurements presented are averages from three individual plants ± SD from independent *LOH1*, *LOH2*, and *LOH3* overexpression lines; lines with the same letter are not significantly different at $P < 0.05$ by Tukey's test ($P = 0.00$ for all LOH2 lines; $P = 0.038$, LOH3 line A; and $P = 0.014$, LOH3 line C, compared with Col-0 by Tukey's test).
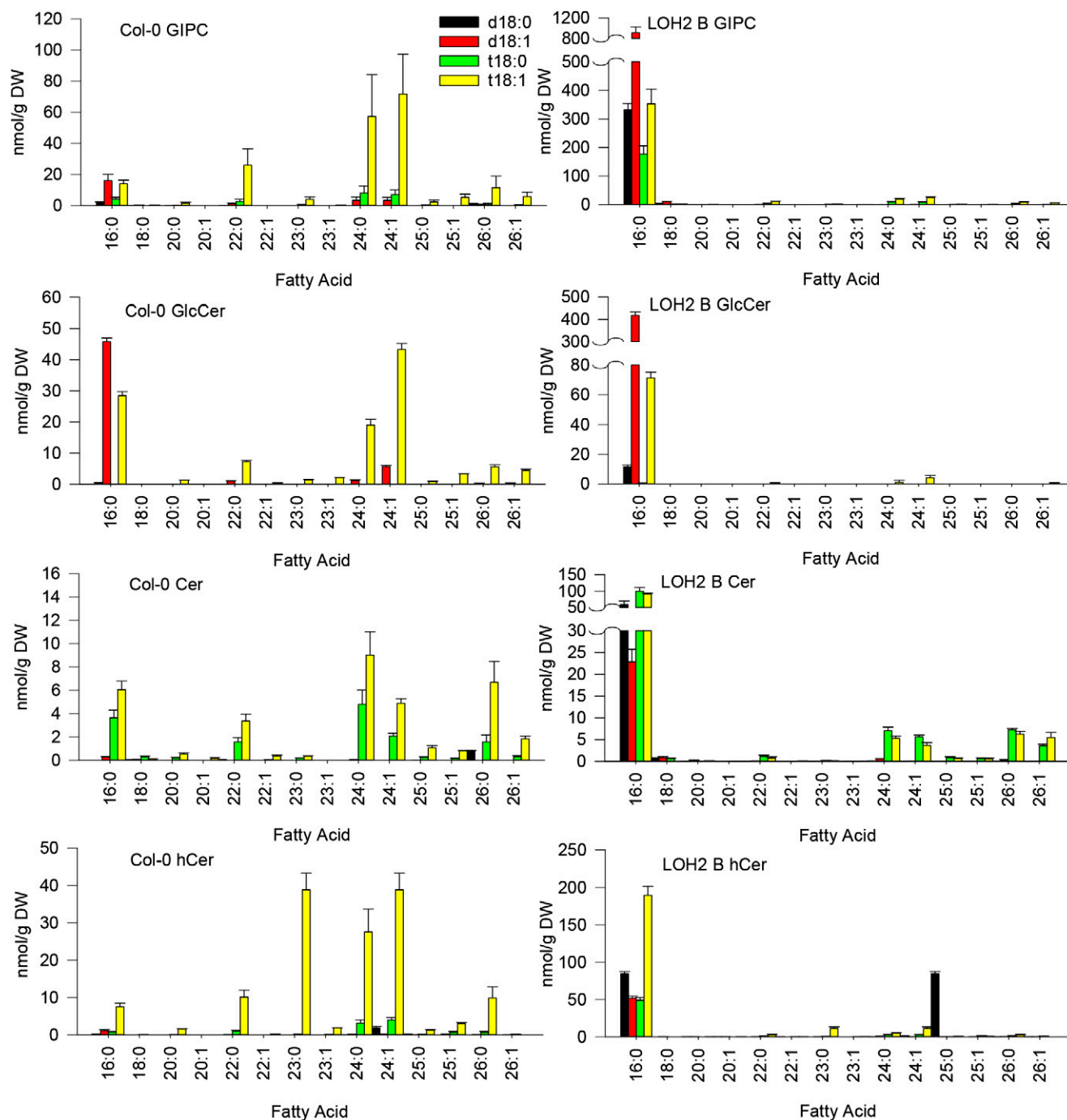
Figure 4. Sphingolipidome of the wild type (Col-0) and *LOH2* overexpression lines. The contents of molecular species of GIPC, GlcCer, ceramide (Cer), and hydroxyceramide (hCer) for Col-0 and a representative *LOH2* line are shown. The data presented are LCB (*y* axis) and fatty acid (*x* axis) concentrations of molecular species as determined by liquid chromatography-electrospray ionization-tandem mass spectrometry analyses. Data shown are averages of measurements of rosettes from 4-week-old plants (*n* = 3 biological replicates ± SD). DW, Dry weight.

Overexpression of *LOH1* and *LOH3* resulted in a significant increase in plant size as determined by the measurement of total dry weight of soil-grown rosettes and hydroponically grown roots at 1 month post germination. These results contrasted with *LOH2* overexpression, which resulted in severe dwarfing and reduced root mass compared with wild-type plants (Fig. 1, A and B). To determine if the difference in plant size was caused by an increase in the number of cells, root meristem cell numbers were determined for 10-d-old representative

LOH1-, *LOH2-*, and *LOH3*-overexpressing lines. *LOH1* and *LOH3* overexpression resulted in a significant increase in cell number of root meristems, while *LOH2* overexpression resulted in a significant decrease in cell number of root meristems (average number of cells ± SE [n = 10], Col-0 = 33.9 ± 1.9, LOH1 line B = 39.4 ± 1.7, LOH2 line A = 24.6 ± 1.4, and LOH3 line C = 47 ± 2.8; Fig. 2A). Representative root meristems are shown in Supplemental Figure S2, A to D. These results indicate that differences in growth can be attributed, at least in part, to increased cell division in *LOH1* and *LOH3* overexpression lines and decreased cell division in *LOH2* overexpression lines.

LOH1, LOH2, and LOH3 Overexpression in Arabidopsis Differentially Alters Sphingolipid Profiles

Sphingolipid profile analyses of *LOH2* overexpression lines revealed an approximately 2.5- to 3.5-fold increase in overall total sphingolipids, almost exclusively composed of molecular species with ceramide backbones containing dihydroxy LCBs and C16 fatty acids (Fig. 3A). In addition, approximately 90% of sphingolipids contained C16 fatty acids in *LOH2* overexpression plants. By comparison, approximately 20% of sphingolipids contained C16 fatty acids in wild-type Arabidopsis (Fig. 3B). The increase in C16 fatty acid/dihydroxy LCB sphingolipids was not limited to any single class but found in the ceramide, hydroxyceramide, GlcCer, and GIPC fractions (Fig. 4). The amount of trihydroxy LCB-containing sphingolipids did not change in any of the LOH2 overexpression lines. In contrast to results from *LOH2* overexpression lines, *LOH1* and *LOH3* overexpression resulted in little change in total sphingolipid content and composition of plants relative to wild-type controls, although small but significant reductions in C16 fatty acid-containing sphingolipids were detected as a result of minor changes throughout the sphingolipidome (Fig. 3; Supplemental Fig. S3).
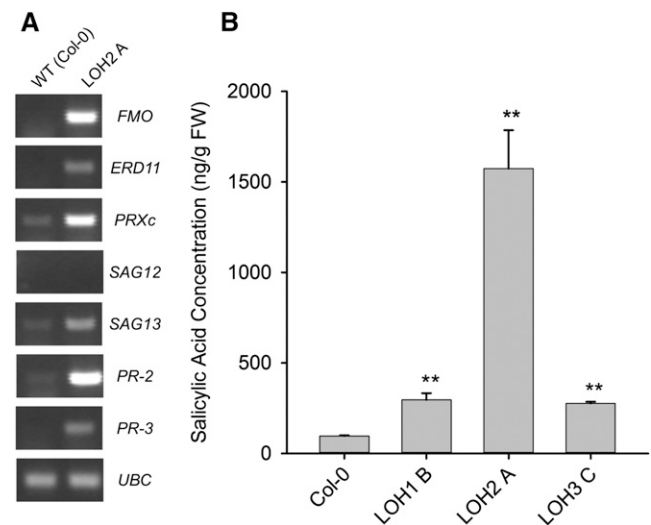
LOH2 Overexpression Enhances Salicylic Acid Production and Induces Hypersensitive Response-Type PCD-Related Genes

The phenotypes described above for *LOH2* overexpression lines, including reduced plant size and enhanced accumulation of sphingolipids, closely resemble those reported previously in mutants and RNA interference suppression lines of the LCB C-4 hydroxylase genes (Chen et al., 2008). Another notable feature of the LCB C-4 hydroxylase *sphingoid base hydroxylase-1 (sbh-1)sbh-2* mutant was the detection of constitutive up-regulation of a number of genes associated with HR-type PCD (Chen et al., 2008). RT-PCR was conducted to determine if constitutive up-regulation of HR-type PCD marker genes is also detectable in *LOH2* overexpression lines. Similar to patterns observed in the *sbh-1sbh-2* mutant (Chen et al., 2008), HR-type PCD marker genes displayed constitutive up-regulation in the *LOH2* overexpression lines. Up-

regulation of the expression of these PCD marker genes, however, was not detected in wild-type, *LOH1*, or *LOH3* overexpression lines (Fig. 5A; Supplemental Fig. S4). Accumulation of salicylic acid in *LOH2* overexpression lines was also indicative of HR-type PCD. Consistent with this, a 16-fold increase in salicylic acid levels was detected in the *LOH2* overexpression line (Fig. 5B). Notably, *LOH1* and *LOH3* overexpression lines had salicylic acid concentrations 3-fold higher for LOH1 B and LOH3 C, respectively (P = 0.007, LOH1 line B; P = 0.000, LOH3 line C) compared with those detected in wild-type plants.

LOH1-, LOH2-, and LOH3-Overexpressing Plants Displayed Different Phenotypes When Grown on FB$_1$

Ceramide synthases are known targets for inhibition by the PCD-inducing mycotoxin. It is generally believed that FB$_1$ cytotoxicity is associated with the accumulation of free LCBs (Abbas et al., 1994). Given that FB$_1$ is regarded as a competitive inhibitor of ceramide synthases, we hypothesized that ceramide synthase overexpression would reduce the cytotoxicity of FB$_1$. To test this, seedlings of wild-type Arabidopsis (Col-0) and

Figure 5. Expression of marker genes for HR-type PCD in the wild type (Col-0) and LOH2 overexpression lines and comparison of salicylic acid concentrations in the wild type (Col-0) and *LOH1*, *LOH2*, and *LOH3* overexpression lines. A, RT-PCR was conducted to assess the expression of PCD marker genes in leaves of 4-week-old wild-type (WT) Col-0 and a representative *LOH2* overexpression line. The PCD marker genes analyzed are *FLAVIN MONOOXYGENASE* (*FMO*; At1g19250), *EARLY RESPONSIVE TO DEHYDRATION11* (*ERD11*; At1g02930), *PEROXIDASEc* (*PRXc*; At3g49120), *SENESCENCE-ASSOCIATED GENE13* (*SAG13*; At2g29350), *SAG12* (At5g45890), *PATHOGENESIS-RELATED GENE2* (*PR2*; At3g57260), and *PR3* (At3g12500). The gene for ubiquitin-conjugating enzyme, *UBC* (At5g25760), was used as a positive control. B, Salicylic acid concentrations were measured in leaves of 4-week-old *LOH1*, *LOH2*, and *LOH3* overexpression lines. Data presented are averages of measurements from three independent plants for each line ± SE (**, P < 0.01; P = 0.002, LOH2 line A). FW, Fresh weight.

overexpression lines of *LOH1*, *LOH2*, or *LOH3* were germinated on medium containing 0.5 μM FB$_1$ and grown for 1 month. In contrast to wild-type controls, plants expressing *LOH2* and *LOH3* were viable on 0.5 μM FB$_1$, whereas *LOH1*-overexpressing plants displayed severely reduced viability similar to wild-type control plants on 0.5 μM FB$_1$ (Fig. 6A). Consistent with these observations, *LOH2*- and *LOH3*-overexpressing plants accumulated approximately 25% of the free and phosphorylated LCB concentrations of wild-type plants grown on 0.5 μM FB$_1$ (Fig. 6B). Total free and phosphorylated LCB concentrations in *LOH1*-overexpressing plants were approximately 50% of those of wild-type plants in the FB$_1$ treatment (Fig. 6B). These results suggest that LOH1 ceramide synthase is more sensitive to inhibition by FB$_1$ than LOH2 and LOH3 ceramide synthases. Sphingolipid compositional analysis of wild-type seedlings grown on plates supplied with FB$_1$ showed increases primarily in C16 fatty acid-containing sphingolipids, including C16 fatty acid-containing ceramides, indicating a preferential inhibition of LOH1 and/or LOH3 ceramide synthases by FB$_1$ (Supplemental Fig. S5). Notably, the accumulation of ceramide with C16 fatty acids was strongly

suppressed in *LOH3*-overexpressing plants relative to wild-type and *LOH1*- and *LOH2*-overexpressing plants. Instead, ceramides in *LOH3* overexpression lines were primarily enriched in VLCFAs (Supplemental Fig. S5).

DISCUSSION

The results presented here demonstrate that enhanced expression of each of the three Arabidopsis ceramide synthase genes has widely differing effects on growth, sphingolipid metabolism, and response to the PCD-inducing mycotoxin FB$_1$. Most strikingly, *LOH2* overexpression resulted in severe dwarfing and the accumulation of sphingolipids enriched in C16 fatty acids and dihydroxy LCBs (Fig. 7). Conversely, overexpression of *LOH1* and *LOH3*, in particular, resulted in plants with significantly increased biomass relative to wild-type control plants but little, if any, alteration in sphingolipid composition or content on a tissue mass basis (Fig. 7). In addition, *LOH2* overexpression was accompanied by constitutive up-regulation of HR-type PCD marker genes and strongly enhanced accumulation of salicylic acid. Furthermore, plants overexpressing *LOH2* and *LOH3* displayed resistance to FB$_1$
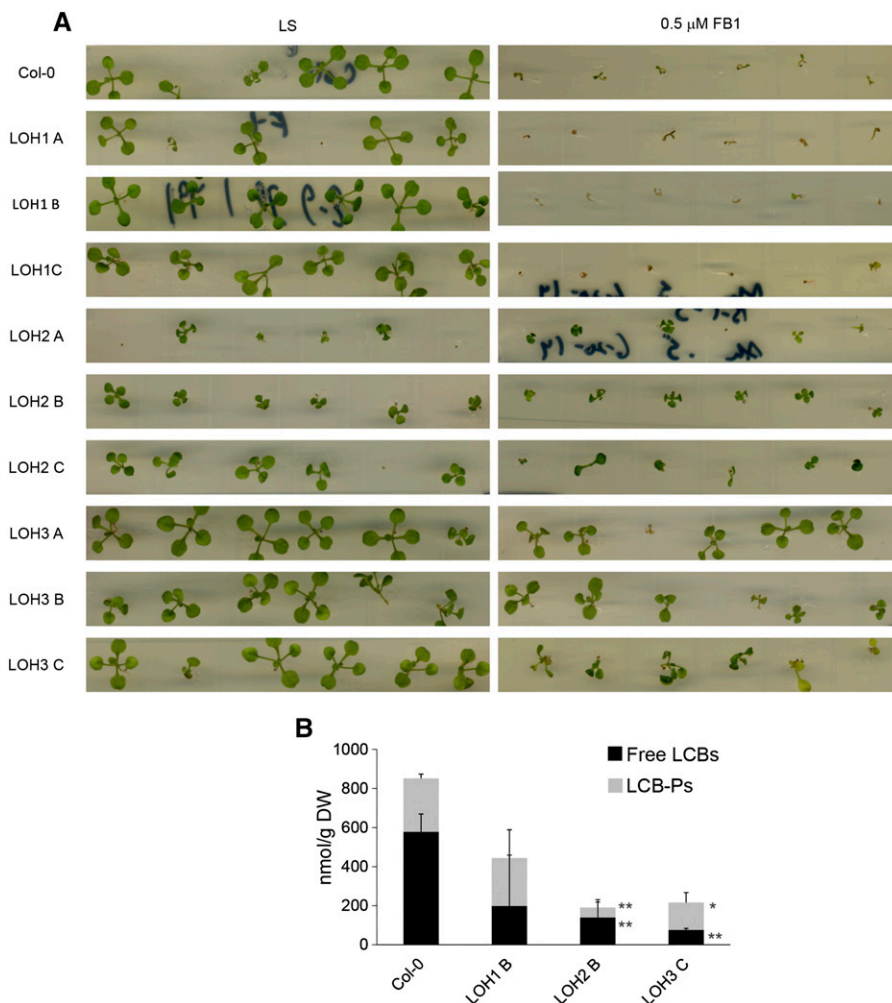
Figure 6. Comparison of responses of the wild type and ceramide synthase overexpression lines to the mycotoxin FB$_1$. A, Comparison of sensitivities of the wild type (Col-0) and selected *LOH1*, *LOH2*, and *LOH3* overexpression lines to FB$_1$. As shown, plants were grown for 4 weeks on Linsmaier and Skoog (LS) medium ± 0.5 μM FB$_1$. B, Free LCBs and LCB-phosphates (LCB-Ps) were measured in 4-week-old plants harvested from FB$_1$-containing plates. Data shown are averages of three biological replicates ± SD for Col-0 and *LOH1*, *LOH2*, and *LOH3* overexpression lines (*, $P < 0.05$ and **, $P < 0.01$; free LCBs-LOH2 line B, $P = 0.00$; LOH3 line C, $P = 0.00$; LCB-Ps-LOH2 line B, $P = 0.00$; LOH3 line C, $P = 0.01$). DW, Dry weight.
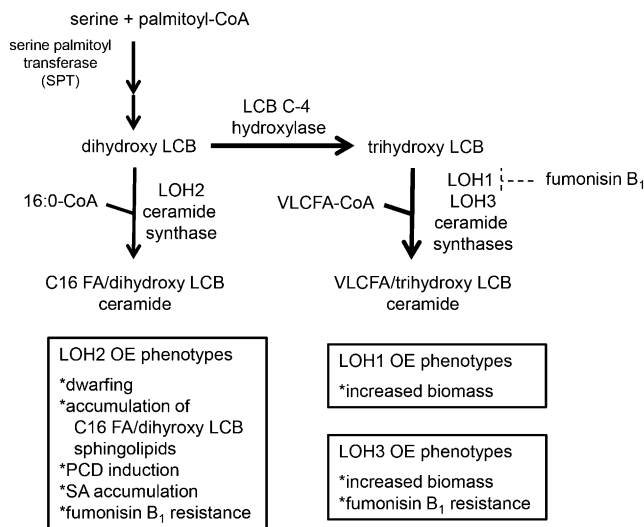
Figure 7. Model of ceramide synthesis and biochemical and physiological outcomes from the overexpression of *LOH1*-, *LOH2*-, and *LOH3*-encoded ceramide synthases. Dihydroxy LCBs originating from Ser palmitoyltransferase (SPT) activity can be linked to C16 fatty acyl-CoA substrates via LOH2 ceramide synthase activity. Alternatively, dihydroxy LCBs can be hydroxylated by LCB C-4 hydroxylase. The resulting trihydroxy LCBs can then be used as substrates for LOH1 and LOH3 ceramide synthases for linkage with VLCFA-CoA substrates. The findings presented suggest that LOH1 ceramide synthase is the most sensitive of the three Arabidopsis ceramide synthases to FB_1 inhibition. FA, Fatty acid; OE, overexpression; SA, salicylic acid.

and had reduced accumulation of free LCBs and LCB-phosphates in response to FB_1 compared with wild-type controls. *LOH1*-overexpressing plants, in contrast, displayed sensitivity to FB_1, and although these lines accumulated approximately 50% lower amounts of free LCBs and LCB-phosphates compared with the wild-type plants, levels of these metabolites were 2-fold or more higher than those in *LOH2* and *LOH3* overexpression plants grown on FB_1-containing medium.

The nearly identical phenotypes for LCB C-4 hydroxylase suppression, described previously (Chen et al., 2008), and LOH2 ceramide synthase overexpression, described here, are consistent with these enzymes catalyzing competing reactions for the metabolism of dihydroxy LCBs (Fig. 7). Based on these findings, functional LCB C-4 hydroxylation combined with the activities of LOH1 and LOH3 ceramide synthases are sufficient for channeling LCBs into ceramides enriched in VLCFAs and trihydroxy LCBs that are capable of supporting growth. It is likely that the high accumulation of ceramides with C16 fatty acids and dihydroxy LCBs in the *LOH2* overexpression lines disrupts the growth-supporting roles of LOH1 and LOH3 ceramide synthase-derived sphingolipids in processes such as Golgi trafficking. Given that LOH2 ceramide synthase products do not support growth and their accumulation induces PCD, it is unclear what the physiological significance of this enzyme is. Consistent with this, *LOH2* mutants do not display phenotypic defects when

maintained under typical growth conditions (Markham et al., 2011; Ternes et al., 2011a). Ultimately, the composition of ceramides in Arabidopsis reflects the combined activities of LOH1, LOH2, and LOH3 ceramide synthases. Publicly available data from microarray studies indicate that *LOH2* is expressed in vegetative organs at similar levels to *LOH1* (Supplemental Fig. S6). *LOH3* is also expressed in vegetative organs but at levels lower than *LOH1* and *LOH2* (Supplemental Fig. S6). Despite the nearly equal expression of *LOH1* and *LOH2*, sphingolipids containing C16 fatty acids arising from LOH2 ceramide synthase activity account for only 20% of total sphingolipid content in rosettes of wild-type plants (Fig. 3B). One possibility to explain this apparent discrepancy in the production of *LOH2*-derived ceramides versus the expression levels of this gene is the competition between the LOH2 ceramide synthase and the LCB C-4 hydroxylase for dihydroxy LCBs. Under normal conditions, greater activity of LCB C-4 hydroxylase may favor the biosynthesis of trihydroxy LCBs that are subsequently incorporated into ceramides by LOH1 and LOH3 ceramide synthases. In such a metabolic scenario, LOH2 ceramide synthase activity may serve as a safety valve to sequester excess LCBs into ceramides as a less cytotoxic form than free LCBs. Supportive of this idea, *LOH2* overexpression resulted in the accumulation of C16 fatty acid/dihydroxy LCB-containing ceramides, but it reduced LCB accumulation that was associated with enhanced resistance to FB_1 (Fig. 6B; Supplemental Fig. S5C). These findings also suggest that FB_1 toxicity is due primarily to the accumulation of free LCBs rather than the accumulation of C16 fatty acid/dihydroxy LCB ceramides. Also consistent with the safety valve function of the LOH2 ceramide synthase is the apparent relative resistance of this enzyme to FB_1 inhibition relative to the LOH1 ceramide synthase (Fig. 6A).

Another notable finding from these studies is the ability of *LOH1* and *LOH3* overexpression to promote increased biomass of Arabidopsis plants (Fig. 1). Despite the up-regulation of *LOH1* and *LOH3* expression, the plants did not have significantly increased levels of sphingolipids on a mass basis (Supplemental Fig. S3). Similarly, it was shown previously that plants with partial suppression of sphingolipid synthesis are dwarfed, but they did not have reduced amounts of sphingolipids on a mass basis (Chen et al., 2006). From these findings, it was proposed that sphingolipid production limits growth (Chen et al., 2006). Our findings here suggest that the converse is also true: enhanced production of ceramides with VLCFAs and trihydroxy LCBs can promote growth. An understanding of the mechanism for this growth promotion and possible translation of these finding for the engineering of crops with increased biomass requires further study. It is known that sphingolipids with VLCFAs are important for Golgi trafficking of proteins to the plasma membrane that are associated with plant growth, including cell wall biosynthetic enzymes and auxin influx and efflux carriers (Bach et al., 2011; Markham et al., 2011). One possibility is that enhanced production of

sphingolipids with VLCFAs drives increased rates of Golgi trafficking in Arabidopsis cells. Sphingolipids with VLCFAs resulting from LOH1 and LOH3 ceramide synthase activities also contribute to cell plate or phragmoplast formation during cell division (Bach et al., 2011; Molino et al., 2014). Consistent with this, our findings show that enhanced growth of *LOH1* and *LOH3* overexpression plants is due in part to increased cell division. It is also possible that enhanced growth results, in part, from increased cell expansion due to targeting of sphingolipids with LOH1 and LOH3 ceramide synthase-derived ceramides to membranes, such as tonoplast and plasma membrane, that contribute directly to cell expansion. Clarification of this possibility awaits reports of the sphingolipid compositional profiling of specific membrane fractions in plant cells.

An additional observation from these studies is that the structural distinction of GlcCer and GIPC ceramides typically found in plants can be altered by *LOH2* overexpression. In Arabidopsis and other plants, GlcCers are enriched in C16 fatty acid/dihydroxy LCB ceramides derived from LOH2 ceramide synthase and GIPCs are enriched in VLCFA/trihydroxy LCB ceramides derived from LOH1 and LOH3 ceramide synthases (Markham et al., 2006). However, ceramides of both GlcCer and GIPC contain predominantly C16 fatty acids and dihydroxy LCBs upon *LOH2* overexpression, a phenotype also observed in LCB C-4 hydroxylase mutants (Chen et al., 2008). This observation may reflect broad ceramide substrate specificity of inositol phosphorylceramide (IPC) synthases, the enzymes that catalyze the initial reaction in GIPC synthesis (Wang et al., 2008; Mina et al., 2010), or impaired sorting of specific ceramides between the endoplasmic reticulum and Golgi bodies, the primary site of IPC and GIPC synthesis (Wang et al., 2008; Rennie et al., 2014), in response to *LOH2* overexpression. This point cannot be addressed at present due to the lack of published information on substrate specificities of IPC synthases and endoplasmic reticulum-Golgi ceramide sorting mechanisms.

Although LOH1 and LOH3 ceramide synthases share nearly 80% amino acid sequence identity, *LOH1* and *LOH3* expression resulted in distinct differences in FB$_1$ sensitivity. In three *LOH1* and *LOH3* independent overexpression lines, *LOH1* overexpression resulted in sensitivity to 0.5 μM FB$_1$, but *LOH3* overexpression resulted in resistance to 0.5 μM FB$_1$ (Fig. 6). In addition, the accumulation of LCBs and LCB-phosphates was more strongly suppressed in the LOH3 C line versus the LOH1 B line, and in contrast to the LOH1 B line, little accumulation of C16 fatty acid-containing ceramides was detected in the LOH3 C line (Fig. 6; Supplemental Fig. S5). Based on these findings, one possibility is that the LOH3 ceramide synthase, like the LOH2 ceramide synthase, is considerably less sensitive to FB$_1$ inhibition than the LOH1 ceramide synthase. Differential sensitivity to FB$_1$ among the LOH1, LOH2, and LOH3 ceramide synthases may also explain why GIPC levels are increased following FB$_1$ treatment of wild-type plants (Supplemental Fig. S5A). In this case, the predominant

GIPC species accumulated were from LOH2 ceramide synthase-type activity. We are currently examining the hypothesis that LOH1, LOH2, and LOH3 ceramide synthases are differentially inhibited by FB$_1$ through in vitro assay of recombinant forms of each enzyme, in the absence or presence of FB$_1$.

Overall, these findings complement those from previous characterizations of LOH1, LOH2, and LOH3 ceramide synthase knockout mutants (Markham et al., 2011; Ternes et al., 2011a) and show that increased expression of the corresponding enzymes can have profound effects on growth, sphingolipid metabolism, PCD induction, and sensitivity to sphinganine-analog mycotoxins. These findings also provide insights into potential targets for crop improvement by tailoring of sphingolipid biosynthesis.

MATERIALS AND METHODS

All chemicals, unless stated otherwise, were purchased from Sigma-Aldrich. All statistical analyses, unless stated otherwise, are represented as the *P* value of Student's *t* test. ANOVA and Tukey's test were performed using the SigmaStat function of SigmaPlot 13.0.

Plant Growth Conditions

Arabidopsis (*Arabidopsis thaliana*) plants were grown on Farfard soil mix (Hummert International) or surface sterilized in 1:1 (v/v) bleach:water for 10 min followed by washing three times with sterile water and grown on LS (Phytotechnology Laboratories) agar plates. Plates were vernalized at 4°C for 48 h after seeds were sown. Soil-grown plants were maintained at 22°C and 50% humidity with a 16-h-light (100 μmol m^{-2} s^{-1})/8-h-dark cycle. Plants sown on LS agar plates were maintained at room temperature under 24 h of light (100 μmol m^{-2} s^{-1}).

Hydroponic plants for root mass were grown essentially as described previously (Conn et al., 2013). Briefly, seeds were sown onto germination medium (1.2 mM K$^+$, 1 mM Ca^{2+}, 1 mM Mg^{2+}, 2.51 mM Cl$^-$, 0.5 mM NO$_3^-$, 1.0105 mM SO$_4^{2-}$, 0.2 mM PO$_4^{2-}$, 0.101 mM Na$^+$, 0.01 mM Fe^{3+}, 0.005 mM Mn^{2+}, 0.01 mM Zn^{2+}, 0.0005 mM Cu^{2+}, and 0.0001 mM Mo^{4+}) plus 0.7% (w/v) agar and vernalized at 4°C for 2 d. Plants were transferred to 22°C and 50% humidity with a 16-h-light (100 μmol m^{-2} s^{-1})/8-h-dark cycle with the germination medium as the hydroponic solution. After 1 week of growth, plants were transferred to a hydroponic solution consisting of 1:1 germination medium and basal medium (5.6 mM K$^+$, 2.1 mM Ca^{2+}, 2 mM Mg^{2+}, 2 mM NH$_4^+$, 3.71 mM Cl$^-$, 9 mM NO$_3^-$, 2.0105 mM SO$_4^{2-}$, 0.6 mM PO$_4^{2-}$, 1.5502 mM Na$^+$, 0.01 mM Fe^{3+}, 0.005 mM Mn^{2+}, 0.01 mM Zn^{2+}, 0.0005 mM Cu^{2+}, and 0.0001 mM Mo^{4+}). After 1 week in a 1:1 (v/v) germination medium:basal medium solution, plants were moved to full basal medium with the hydroponic solution changed weekly.

Overexpression and Col-0 plants were plated as described above onto LS plates with and without FB$_1$ (5 μM). Four weeks after germination, plants were harvested and lyophilized overnight for sphingolipidomic analyses.

Plant Transformation

LOH1 and *LOH3* cDNAs were amplified by PCR using oligonucleotide primer sets P1 and P3 (Supplemental Table S1) and Phusion polymerase (New England Biolabs) from an Arabidopsis cDNA library prepared from flowers (Paul et al., 2006). *LOH1* and *LOH3* PCR products were cloned into the *Eco*RI-*Xba*I restriction sites of the binary vector pBinRed35S downstream of the CaMV 35S promoter. The *LOH2* cDNA was amplified by PCR using the oligonucleotide primer set P2 (Supplemental Table S1) and cloned into pENTR/D-TOPO (Invitrogen) vector. The vector was linearized using *Apa*I, gel purified, and used to conduct an LR reaction with the binary vector pCD3-724-Red (pEarlyGate100 modified to contain the DsRed selection; Earley et al., 2006). The binary vectors harboring each cDNA under the control of the CaMV 35S promoter were introduced in *Agrobacterium tumefaciens* C58 by electroporation. Transgenic plants were created by floral dip of Arabidopsis (Col-0; Clough and Bent, 1998). Seeds were screened with a green light-emitting diode and a Red2 camera filter to identify transformed seeds based on DsRed fluorescence (Jach et al., 2001). Seeds were planted in soil and maintained under 22°C and 50% humidity with a

16-h-light (100 μmol m^{-2} s^{-1})/8-h-dark cycle through three or more generations to obtain homozygous lines for phenotypic characterization.

Transgene Expression Analyses

For analyses of *LOH1* and *LOH2* overexpression levels, total RNA was extracted from leaves of 4-week-old Arabidopsis wild-type (Col-0) and overexpression plants. RNA extraction was performed using the RNeasy Plant Kit (Qiagen) according to the manufacturer's protocol. Total RNA (1 μg) was treated with DNaseI (Invitrogen) according to the manufacturer's protocol. Treated RNA was then reverse transcribed to cDNA with the iScript cDNA synthesis kit (Bio-Rad) according to the manufacturer's protocol. Quantitative PCR (qPCR) was performed on the cDNA using the Bio-Rad MyiQ iCycler qPCR instrument. SYBR Green was used as the fluorophore in a qPCR supermix (Qiagen). QuantiTect (Qiagen) primer sets for *LOH1* (QT00779331) and *LOH2* (QT00774949) were used for relative quantification, with *protein phosphatase 2A subunit A3* gene (*PP2AA3*; At1g13320) used as an internal reference gene.

Because of difficulties obtaining qPCR signals for *LOH3* using the QuantiTect primer set, northern-blot analysis of *LOH3* expression was carried out as described previously (Buhr et al., 2002). Briefly, RNA was isolated using the RNeasy Plant Kit (Qiagen) according to the manufacturer's protocol. A total of 8.5 μg of RNA was separated on a 1% (v/v) formaldehyde agarose gel. The separated RNA was subsequently transferred to a nylon membrane (Zeta Probe GT; Bio-Rad) and fixed by UV light cross-linking. Probes, approximately 50 ng, were made by digesting LOH3 cDNA out of the plant transformation construct and were labeled with [^{32}P] dCTP by random primer synthesis (Prime-It II Random Synthesis Kit; Agilent Technologies). The membrane was hybridized in a solution of 1 mM EDTA, 0.5 M Na$_2$HPO$_4$ (pH 7.2), 7% (w/v) SDS, and 1% (w/v) bovine serum albumin at 65°C overnight. The membrane was washed twice with 5% (w/v) SDS and 40 mM Na$_2$HPO$_4$ solution for 30 min at 65°C, with a subsequent third wash with 1% (w/v) SDS and 40 mM Na$_2$HPO$_4$ solution for 30 min at 65°C after hybridization. The membrane was exposed on x-ray film for 2 h to 2 d at −80°C. After development, the membrane was stripped by incubating two times in 0.1× SSC/0.5% (w/v) SDS at 95°C for 20 min and reprobed for expression of the ubiquitin-conjugating enzyme gene (At5g25760) as a loading control. The probe was made as described above, with the cDNA source coming from PCR amplification from an Arabidopsis flower cDNA library using oligonucleotide primer set P4 (Supplemental Table S1).

Sphingolipidomic Analysis

Sphingolipids were extracted from 2 to 30 mg of approximately 4-week-old plants as described previously (Markham and Jaworski, 2007). Sphingolipid profiling by liquid chromatography-electrospray ionization-tandem mass spectrometry was performed as described (Markham and Jaworski, 2007). Binary gradients were generated as described (Markham and Jaworski, 2007) using tetrahydrofuran:methanol:5 mM ammonium formate (3:2:5 [v/v]) plus 0.1% (v/v) formic acid (solvent A) and tetrahydrofuran:methanol:5 mM ammonium formate (7:2:1 [v/v]) plus 0.1% (v/v) formic acid (solvent B). Sphingolipids were detected using a 4000 QTRAP mass spectrometer (AB SCIEX) with instrument settings as described previously (Markham and Jaworski, 2007). Multiple reaction monitoring transitions and data analysis using Analyst 1.5 and Multiquant 2.1 software (AB SCIEX) were performed as described by Markham and Jaworski (2007).

Total LCB Analysis

Total LCB content was analyzed by HPLC as described previously (Markham et al., 2006). Briefly, approximately 10 mg of lyophilized plant material was hydrolyzed for 14 h at 110°C in 10% (w/v) barium hydroxide:dioxane (1:1, v/v). Following hydrolysis, samples were treated with 2 volumes of 2% (w/v) ammonium sulfate to remove barium ions and 2 volumes of diethyl ether to extract the released LCBs. The upper layer was transferred to a 13- × 100-mm glass screw-capped tube and dried under N$_2$ at 60°C, derivatized with *ortho*-phthalaldehyde, and analyzed as described previously by Markham et al. (2006).

Total Dry Weight Analysis

Four-week-old soil-grown plants were harvested by cutting the root just below the rosette and removing any flower bolts, if present. The harvested tissue was frozen in liquid N$_2$ and lyophilized overnight. For root mass, hydroponically grown plants were cut just under the rosette, and roots were frozen in liquid N$_2$ and lyophilized overnight.

Root Meristem Imaging and Cell Number Measurement

Plants were sown onto LS medium as described above and grown vertically under 24 h of light (100 μmol m^{-2} s^{-1}). Roots at 10 d post germination were harvested and fixed in 4% (v/v) paraformaldehyde in 1× phosphate-buffered saline and stored at 4°C. Roots were stained with propidium iodide (10 μg mL^{-1}) for approximately 2 min and washed with 1× phosphate-buffered saline. Images were taken using the Nikon A1 confocal microscope using the NIS-Elements 4.20.01 acquisition software. Propidium iodide images were acquired with a 561.4-nm excitation and an emission of 570 to 620 nm. Images were taken at 20× magnification. Cells located in the first continuous root epidermal layer were counted from the cell plate just above the quiescent center to the first fully differentiated cell (identified by the first cell that is approximately double the size of the previous cell) using the cell counter function of Fiji ImageJ.

RT-PCR of PCD-Related Genes

Total RNA was extracted from 4-week-old Col-0 and *LOH2* overexpression plants, and first strand cDNA was prepared as described above. Semiquantitative RT-PCR analysis was conducted with equal amounts of first strand cDNA as template. Oligonucleotide primer sets and the numbers of PCR cycles used for each target gene are provided in Supplemental Table S1 (P5-11). Gene expression was analyzed for *FMO* (At1g19250), *ERD11* (At1g02930), *PRXc* (At3g49120), *SAG13* (At2g29350), *SAG12* (At5g45890), *PR2* (At3g57260), and *PR3* (At3g12500). *UBC* (P4; At5g25760) expression was measured as an internal positive control as described previously (Brodersen et al., 2002; Chen et al., 2008).

Salicylic Acid Measurements

Free salicylic acid was quantitated by electrospray ionization-tandem mass spectrometry using the method of Pan et al. (2010) with modifications. Five nanograms of 2-hydroxybenzoic acid-[^{2}H$_6$]d$_6$-salicylic acid per 50 mg of tissue was added as an internal standard. Extracts were resuspended in 100 μL of methanol and 500 μL of column buffer A (water/0.1% [v/v] formic acid/0.3 mM ammonium formate), injected onto a 100- × 2.1-mm Agilent Eclipse Plus C18 column (3.5-μm particle size) with holding at 25% B (water:acetonitrile [10:90] containing 0.1% [v/v] formic acid and 0.3 mM ammonium formate) for 1 min, and eluted with a 5-min gradient formed by 45% to 95% B at a flow rate of 0.25 mL min^{-1}. In this system, free salicylic acid and the deuterated standard elute at 3.8 min. Ions were detected using previously published multiple reaction monitoring (Pan et al., 2010) by a QTRAP 4000 triple quadrupole mass spectrometer operated in negative mode, with instrument settings optimized first using standards. Quantitation based on comparison of analyte and standard peak areas was done using Multiquant 2.1 software (AB SCIEX).

Supplemental Data

The following supplemental materials are available.

Supplemental Figure S1. Expression levels of *LOH1* and *LOH2* in leaves of independent overexpression lines.

Supplemental Figure S2. Representative root meristem region for measurement of cell numbers.

Supplemental Figure S3. Sphingolipidomes of *LOH1* and *LOH3* overexpression lines.

Supplemental Figure S4. Expression of marker genes for hypersensitive response programmed cell death.

Supplemental Figure S5. Sphingolipidomes of FB$_1$-treated plants.

Supplemental Figure S6. Gene expression levels of *LOH1*, *LOH2*, and *LOH3* in different organs.

Supplemental Table S1. Oligonucleotides used for cloning and marker gene expression measurements.

LITERATURE CITED

Abbas HK, Tanaka T, Duke SO, Porter JK, Wray EM, Hodges L, Sessions AE, Wang E, Merrill AH Jr, Riley RT (1994) Fumonisin- and AAL-toxin-induced disruption of sphingolipid metabolism with accumulation of free sphingoid bases. Plant Physiol 106: 1085–1093

Bach L, Gissot L, Marion J, Tellier F, Moreau P, Satiat-Jeunemaître B, Palauqui JC, Napier JA, Faure JD (2011) Very-long-chain fatty acids are required for cell plate formation during cytokinesis in Arabidopsis thaliana. J Cell Sci 124: 3223–3234

Bi FC, Liu Z, Wu JX, Liang H, Xi XL, Fang C, Sun TJ, Yin J, Dai GY, Rong C, et al (2014) Loss of ceramide kinase in Arabidopsis impairs defenses and promotes ceramide accumulation and mitochondrial H₂O₂ bursts. Plant Cell 26: 3449–3467

Borner GH, Sherrier DJ, Weimar T, Michaelson LV, Hawkins ND, Macaskill A, Napier JA, Beale MH, Lilley KS, Dupree P (2005) Analysis of detergent-resistant membranes in Arabidopsis: evidence for plasma membrane lipid rafts. Plant Physiol 137: 104–116

Brodersen P, Petersen M, Pike HM, Olszak B, Skov S, Odum N, Jørgensen LB, Brown RE, Mundy J (2002) Knockout of Arabidopsis ACCELERATED-CELL-DEATH11 encoding a sphingosine transfer protein causes activation of programmed cell death and defense. Genes Dev 16: 490–502

Buhr T, Sato S, Ebrahim F, Xing A, Zhou Y, Mathiesen M, Schweiger B, Kinney A, Staswick P, Clemente T (2002) Ribozyme termination of RNA transcripts down-regulate seed fatty acid genes in transgenic soybean. Plant J 30: 155–163

Chen M, Cahoon E, Saucedo-García M, Plasencia J, Gavilanes-Ruíz M (2010) Plant sphingolipids: structure, synthesis and function. In H Wada, N Murata, eds, Lipids in Photosynthesis, Vol 30. Springer, Dordrecht, The Netherlands, pp 77–115

Chen M, Han G, Dietrich CR, Dunn TM, Cahoon EB (2006) The essential nature of sphingolipids in plants as revealed by the functional identification and characterization of the Arabidopsis LCB1 subunit of serine palmitoyltransferase. Plant Cell 18: 3576–3593

Chen M, Markham JE, Dietrich CR, Jaworski JG, Cahoon EB (2008) Sphingolipid long-chain base hydroxylation is important for growth and regulation of sphingolipid content and composition in Arabidopsis. Plant Cell 20: 1862–1878

Clough SJ, Bent AF (1998) Floral dip: a simplified method for Agrobacterium-mediated transformation of Arabidopsis thaliana. Plant J 16: 735–743

Conn SJ, Hocking B, Dayod M, Xu B, Athman A, Henderson S, Aukett L, Conn V, Shearer MK, Fuentes S, et al (2013) Protocol: optimising hydroponic growth systems for nutritional and physiological analysis of Arabidopsis thaliana and other plants. Plant Methods 9: 4

Dunn TM, Lynch DV, Michaelson LV, Napier JA (2004) A post-genomic approach to understanding sphingolipid metabolism in Arabidopsis thaliana. Ann Bot (Lond) 93: 483–497

Earley KW, Haag JR, Pontes O, Opper K, Juehne T, Song K, Pikaard CS (2006) Gateway-compatible vectors for plant functional genomics and proteomics. Plant J 45: 616–629

Jach G, Binot E, Frings S, Luxa K, Schell J (2001) Use of red fluorescent protein from Discosoma sp. (dsRED) as a reporter for plant gene expression. Plant J 28: 483–491

Laviad EL, Albee L, Pankova-Kholmyansky I, Epstein S, Park H, Merrill AH Jr, Futerman AH (2008) Characterization of ceramide synthase 2: tissue distribution, substrate specificity, and inhibition by sphingosine 1-phosphate. J Biol Chem 283: 5677–5684

Liang H, Yao N, Song JT, Luo S, Lu H, Greenberg JT (2003) Ceramides modulate programmed cell death in plants. Genes Dev 17: 2636–2641

Markham JE, Jaworski JG (2007) Rapid measurement of sphingolipids from Arabidopsis thaliana by reversed-phase high-performance liquid chromatography coupled to electrospray ionization tandem mass spectrometry. Rapid Commun Mass Spectrom 21: 1304–1314

Markham JE, Li J, Cahoon EB, Jaworski JG (2006) Separation and identification of major plant sphingolipid classes from leaves. J Biol Chem 281: 22684–22694

Markham JE, Molino D, Gissot L, Bellec Y, Hématy K, Marion J, Belcram K, Palauqui JC, Satiat-Jeunemaître B, Faure JD (2011) Sphingolipids containing very-long-chain fatty acids define a secretory pathway for specific polar plasma membrane protein targeting in Arabidopsis. Plant Cell 23: 2362–2378

Mina JG, Okada Y, Wansadhipathi-Kannangara NK, Pratt S, Shams-Eldin H, Schwarz RT, Steel PG, Fawcett T, Denny PW (2010) Functional analyses of differentially expressed isoforms of the Arabidopsis inositol phosphorylceramide synthase. Plant Mol Biol 73: 399–407

Mizutani Y, Kihara A, Igarashi Y (2005) Mammalian Lass6 and its related family members regulate synthesis of specific ceramides. Biochem J 390: 263–271

Mizutani Y, Kihara A, Igarashi Y (2006) LASS3 (longevity assurance homologue 3) is a mainly testis-specific (dihydro)ceramide synthase with relatively broad substrate specificity. Biochem J 398: 531–538

Molino D, Van der Giessen E, Gissot L, Hématy K, Marion J, Barthelemy J, Bellec Y, Vernhettes S, Satiat-Jeunemaître B, Galli T, et al (2014) Inhibition of very long acyl chain sphingolipid synthesis modifies membrane dynamics during plant cytokinesis. Biochim Biophys Acta 1842: 1422–1430

Mortimer JC, Yu X, Albrecht S, Sicilia F, Huichalaf M, Ampuero D, Michaelson LV, Murphy AM, Matsunaga T, Kurz S, et al (2013) Abnormal glycosphingolipid mannosylation triggers salicylic acid-mediated responses in Arabidopsis. Plant Cell 25: 1881–1894

Mullen TD, Hannun YA, Obeid LM (2012) Ceramide synthases at the centre of sphingolipid metabolism and biology. Biochem J 441: 789–802

Pan X, Welti R, Wang X (2010) Quantitative analysis of major plant hormones in crude plant extracts by high-performance liquid chromatography-mass spectrometry. Nat Protoc 5: 986–992

Paul S, Gable K, Beaudoin F, Cahoon E, Jaworski J, Napier JA, Dunn TM (2006) Members of the Arabidopsis FAE1-like 3-ketoacyl-CoA synthase gene family substitute for the Elop proteins of Saccharomyces cerevisiae. J Biol Chem 281: 9018–9029

Rennie EA, Ebert B, Miles GP, Cahoon RE, Christiansen KM, Stonebloom S, Khatab H, Twell D, Petzold CJ, Adams PD, et al (2014) Identification of a sphingolipid α-glucuronosyltransferase that is essential for pollen function in Arabidopsis. Plant Cell 26: 3314–3325

Riebeling C, Allegood JC, Wang E, Merrill AH Jr, Futerman AH (2003) Two mammalian longevity assurance gene (LAG1) family members, trh1 and trh4, regulate dihydroceramide synthesis using different fatty acyl-CoA donors. J Biol Chem 278: 43452–43459

Saucedo-García M, Guevara-García A, González-Solís A, Cruz-García F, Vázquez-Santana S, Markham JE, Lozano-Rosas MG, Dietrich CR, Ramos-Vega M, Cahoon EB, et al (2011) MPK6, sphinganine and the LCB2a gene from serine palmitoyltransferase are required in the signaling pathway that mediates cell death induced by long chain bases in Arabidopsis. New Phytol 191: 943–957

Simanshu DK, Zhai X, Munch D, Hofius D, Markham JE, Bielawski J, Bielawska A, Malinina L, Molotkovsky JG, Mundy JW, et al (2014) Arabidopsis ACCELERATED-CELL-DEATH11, ACD11, is a ceramide-1-phosphate transfer protein and intermediary regulator of phytoceramide levels. Cell Reports 6: 388–399

Sperling P, Franke S, Lüthje S, Heinz E (2005) Are glucocerebrosides the predominant sphingolipids in plant plasma membranes? Plant Physiol Biochem 43: 1031–1038

Ternes P, Feussner K, Werner S, Lerche J, Iven T, Heilmann I, Riezman H, Feussner I (2011a) Disruption of the ceramide synthase LOH1 causes spontaneous cell death in Arabidopsis thaliana. New Phytol 192: 841–854

Ternes P, Wobbe T, Schwarz M, Albrecht S, Feussner K, Riezman I, Cregg JM, Heinz E, Riezman H, Feussner I, et al (2011b) Two pathways of sphingolipid biosynthesis are separated in the yeast Pichia pastoris. J Biol Chem 286: 11401–11414

Venkataraman K, Riebeling C, Bodennec J, Riezman H, Allegood JC, Sullards MC, Merrill AH Jr, Futerman AH (2002) Upstream of growth and differentiation factor 1 (uog1), a mammalian homolog of the yeast longevity assurance gene 1 (LAG1), regulates N-stearoyl-sphinganine (C18-(dihydro)ceramide) synthesis in a fumonisin B1-independent manner in mammalian cells. J Biol Chem 277: 35642–35649

Verhoek B, Haas R, Wrage K, Linscheid M, Heinz E (1983) Lipids and enzymatic-activities in vacuolar membranes isolated via protoplasts from oat primary leaves. Z Naturforsch C 38: 770–777

Wang W, Yang X, Tangchaiburana S, Ndeh R, Markham JE, Tsegaye Y, Dunn TM, Wang GL, Bellizzi M, Parsons JF, et al (2008) An inositolphosphorylceramide synthase is involved in regulation of plant programmed cell death associated with defense in Arabidopsis. Plant Cell 20: 3163–3179

Yang H, Richter GL, Wang X, Młodzińska E, Carraro N, Ma G, Jenness M, Chao DY, Peer WA, Murphy AS (2013) Sterols and sphingolipids differentially function in trafficking of the Arabidopsis ABCB19 auxin transporter. Plant J 74: 37–47